



## Research article

# MHD radiative nanofluid flow induced by a nonlinear stretching sheet in a porous medium

Ahmad Banji Jafar <sup>a,b</sup>, Sharidan Shafie <sup>b</sup>, Imran Ullah <sup>c,\*</sup>

<sup>a</sup> Department of Mathematics, Kebbi State University of Science and Technology, Aliero, P.M.B. 1144, Birnin Kebbi, Kebbi State, Nigeria

<sup>b</sup> Department of Mathematical Sciences, Faculty of Science, Universiti Teknologi Malaysia, 81310 Skudai, Johor Bahru, Malaysia

<sup>c</sup> College of Civil Engineering, National University of Sciences and Technology, 44000, Islamabad, Pakistan



## ARTICLE INFO

## Keywords:

Mechanical engineering  
Nonlinear stretching sheet  
Nanoparticle volume fraction  
Viscous dissipation  
Thermal radiation  
Heat generation  
Porous medium

## ABSTRACT

In this article, we numerically investigate the influence of thermal radiation and heat generation on the flow of an electrically conducting nanofluid past a nonlinear stretching sheet through a porous medium with frictional heating. The partial differential equations governing the flow problems are reduced to ordinary differential equations via similarity variables. The reduced equations are then solved numerically with the aid of Keller box method. The influence of physical parameters such as nanoparticle volume fraction  $\phi$ , permeability parameter  $K$ , nonlinear stretching sheet parameter  $n$ , magnetic field parameter  $M$ , heat generation parameter  $Q$  and Eckert number  $Ec$  on the flow field, temperature distribution, skin friction and Nusselt number are studied and presented in graphical illustrations and tabular forms. The results obtained reveal that there is an enhancement in the rate of heat transfer with the rise in nanoparticle volume fraction and permeability parameter. The temperature distribution is also influenced with the presence of  $K$ ,  $Q$ ,  $R$  and  $\phi$ . This shows that the solid volume fraction of nanoparticle can be used in controlling the behaviours of heat transfer and nanofluid flows.

## 1. Introduction

The effectiveness of the performance of heat transfer rely on the behaviour of thermal conductivity of the working fluid. Thus, the enhancement of the thermal conductivity of the working fluids, such as water, ethyl glycol and oil by suspending a little fraction of nanoparticle (such as Cu, Ag, TiO<sub>2</sub> and Al<sub>2</sub>O<sub>3</sub>) into it form a new class of engineering fluid known as nanofluid [1]. Nanofluid is an innovative way of improving the characteristics of rate of heat transfer and is so attractive due to its numerous industrial, biomedical, electronics, transportation applications, such as in the hybrid-power engine, advanced nuclear system, auto-mobiles, biological sensors and drug delivery [2]. The size of the suspended nanoparticle in diameter is often between 1 and 100 nm and when suspended in the convective fluid will produce a dramatic enhancement in the thermophysical properties of the convective fluid. However, the quest to enhance the rate of cooling/heating creates a lot of advantages in the industrial process such as energy savings, reducing the processing time and the cost of the production.

In view of this, Choi [1] incorporates a solid nanoparticle into the working conventional fluid with the aim that the new fluid formed will possess high thermal conductivity as compared to the usual con-

vectional fluid. He termed the mixture of these nanoparticles and the conventional base fluid as 'nanofluid'. Later, Xuan and Li [3] studied the mixture of Cu nanoparticle and distilled water and reported that the thermal conductivity of the water-based Cu nanofluid is higher than that of distilled water in the ratio of about 1.24 to 1.78. Furthermore, Choi et al. [4] noticed that, a little addition of small amount of solid nanoparticle into convective heat transfer liquid increases the characteristics of thermal conductivity of the convective liquids for about 200%.

In 2006, a comprehensive investigation on convective transport system in nanofluid was reported by Buongiorno [5]. He observed that Brownian diffusion and thermophoresis are the major mechanisms for the enhancement of heat transfer and concluded that the large variations of the temperature in the boundary layer region caused the significant reduction in the fluid viscosity which consequently leads to an increase in the coefficient of heat transfer.

Later in 2007, Tiwari and Das [6] developed another model for the study of nanofluid and heat transfer inside a two-sided lid-driven square cavity by studying the behaviour of nanoparticle volume fraction. They noticed that, the nanoparticle volume fraction is a vital parameter for understanding the influence of the nanoparticle in the fluid flow and

\* Corresponding author.

E-mail address: ullahimran14@gmail.com (I. Ullah).

<https://doi.org/10.1016/j.heliyon.2020.e04201>

Received 11 November 2019; Received in revised form 3 February 2020; Accepted 8 June 2020

heat transfer. Thus, nanoparticle volume fraction is an important parameter in studying the impact and characteristics of nanoparticle on the fluid flow velocity and temperature field. However, Yang et al. [7], reported that the thermal conductivity of nanofluid flow is highly depends on the nanoparticle volume fraction and its properties such as the diameter and the shape.

Khan and Pop [8] was first to analyze the behaviour of nanofluid flow past a stretching sheet using Buongiorno’s model. They concluded that, the rate of heat transfer diminished with the rise in Brownian diffusion and thermophoresis parameters. Subsequently, Khan and Pop [8]’s work was extended by Rana and Bhargava [9]. They numerically addressed the steady viscous nanofluid flow over a nonlinear stretching sheet using finite element method (FEM). A suitable similarity transformation was employed on the governing equations that determines the nanofluid flow. It was observed in their results that an increase in Brownian motion and thermophoresis parameters enhanced the thermal boundary layer thickness. Furthermore, the similarity solution of viscous boundary layer flow of nanofluid past a nonlinear stretching sheet was numerically addressed by Hamad and Ferdows [10] using Tiwari and Das model. The effects of nanoparticle volume fraction and nonlinear stretching sheet parameter were analyzed and it was showed that the presence of nanoparticles in the based fluid is capable of changing the pattern and the behaviour of the fluid flow. Similarly, Hady et al. [11] numerically investigates the influence of radiation on nanofluid flow past a nonlinear stretching surface in the presence of variable wall temperature. They observed that the temperature of the nanofluid reduces with the increase in nonlinear stretching sheet and radiation parameters. Also, Das [12] examined nanofluid flow past a nonlinear stretching sheet by taking into account the prescribed temperature at the surface in the presence of partial condition effect. It was showed that, an increased in nonlinear stretching sheet parameter and slip parameter decreased the nanofluid velocity and increased the thickness of the boundary layer. In the same vein, three dimensional nanofluid flow past a nonlinear stretching sheet was examined by Khan et al. [13] using the fourth-fifth-order Runge-Kutta method. However, a stagnation-point nanofluid flow past a nonlinear stretching sheet with suction/injection was studied by Malvandi et al. [14]. They show that the heat transfer rate is increased with the increased in suction parameter and reduces with the increased in the blowing parameter. Similarly, the effect of thermophoresis and Brownian movement on third-grade nanofluid and heat transfer past an oscillatory moving sheet was examined by Khan et al. [15]. They noticed that Brownian and thermophoresis parameters plays a vital role in enhancing the nanoparticle and that the coefficient of skin friction reduced by augmenting the non-Newtonian fluid parameter.

The study of an electrically conducting nanofluid have also received a significant attention by many authors [16, 17, 18, 19, 20, 21] due to its importance in engineering and technological process such as in the plasma studies, MHD generators, MHD pumps, nuclear reactors, extraction of geothermal energy and bearings. Additionally, considerable attention has also been paid to either the viscous dissipation, thermal radiation or heat generation effects on the boundary layer flow of nanofluid and the characteristics of heat transfer embedded in a porous medium. This process has its extensive applications in oil reservoir and geothermal engineering. Magnetohydrodynamic viscous flow over an exponentially stretching surface with radiative effect in a porous medium was analyzed by Ahmed et al. [22]. Shan et al. [23] Analytically studied Williamson liquid film fluid flow and heat transfer in the presence of thermal radiation through a porous media over linear stretching sheet. They noted in their report that an increase in the porosity parameter reduces the flow of thin films and that liquid film flow is affected by the Lorentz force. Zeeshan et al. [24] also examined MHD boundary layer flow of nanofluids in a porous medium. The effect of thermal radiation and heat generation on convective nanofluid flow past a stagnation point in a porous medium was examined by Pal and Mandal [25]. Rama and Chandra [26] uses

**Table 1**  
Thermophysical properties of water and Cu nanoparticles [30].

Physical properties	Base fluid (water)	Cu (nanoparticle)
$\rho$ (kg/m <sup>3</sup> )	997.1	8933
$C_p$ (J/kg K)	4179	385
$k$ (W/m K)	0.613	400
$\beta \times 10^5$ (K <sup>-1</sup> )	21	1.67
$\sigma$ ( $\Omega.m$ ) <sup>-1</sup>	0.05	$5.96 \times 10^7$

hybrid approach to numerically study the influence of viscous dissipation on magnetohydrodynamic boundary layer nanofluid flow past a nonlinear stretching sheet saturated in a porous medium. Recently, Haroun et al. [27] uses the method of spectral relaxation to study the effect of chemical reaction, viscous dissipation and radiation on magnetohydrodynamic nanofluid flow in a porous medium and noticed that velocity field reduced with the increase in the porosity parameter, while the temperature distributions increased with the increase in porosity parameter. Similarly, magnetohydrodynamic nanofluid flow and heat transfer between porous surface and stretching sheet was analyzed by Geng et al. [28]. Furthermore, Patel [29] examined the impacts of heat generation, nonlinear thermal radiation and cross diffusion on an electrically conducting Casson fluid saturated in a porous medium using homotopy analysis. He noted from his results that the skin friction can be reduced with decrease in the value of magnetic field, Casson fluid and chemical reaction parameters.

The main aim of this work in view of the significance of nanoparticle volume fraction in enhancing the thermal conductivity of the nanofluid flow, is studying the combined effects of thermal radiation, heat generation and viscous dissipation on boundary layer flow using Tiwari and Das mathematical model for convective transport of an electrically conducting nanofluid over a nonlinear stretching sheet through a porous medium. The governing equations was transformed into system of ordinary differential equations via similarity solutions and then solved numerically using Keller box method.

**2. Formulation of the problem**

A steady two-dimensional magnetohydrodynamic nano-fluid flow past a nonlinear stretching sheet saturated in a porous medium in the presence of viscous dissipation, thermal radiation and heat generation using Tiwari and Das model is considered in this article. Water is utilised as the based fluid and Copper as the nanoparticle. It is assumed that the convectonal base fluid and the suspended nanoparticles are assumed to be in thermal equilibrium. The thermophysical properties of the nanofluid are presented in Table 1. The variable stretching velocity, the variable magnetic field and the variable permeability of the porous medium of the nanofluid flow is assumed to be of the form  $U_w = ax^n$ ,  $B(x) = B_0x^{2n-1}$  and  $k(x) = k_0x^{1-n}$  respectively [26], where  $n$  is the stretching sheet parameter,  $a$  is the stretching constant,  $k_0$  is the permeability constant and  $B_0$  is the constant of the magnetic field. The surface of the stretching sheet is also held at a temperature  $T_w = T_\infty + bx^{2n-1}$ , where  $n$  is the parameter for the surface temperature,  $b(> 0)$  is a constant and  $T_\infty$  is the ambient temperature of the nanofluid. The two-dimensional continuity, momentum and energy equations that governed the flow problem can be expressed as, [6, 11, 26]

$$\frac{\partial u}{\partial x} + \frac{\partial v}{\partial y} = 0, \tag{1}$$

$$\rho_{nf} \left( u \frac{\partial u}{\partial x} + v \frac{\partial u}{\partial y} \right) = \mu_{nf} \frac{\partial^2 u}{\partial y^2} - \frac{\mu_{nf}}{k(x)} u - \sigma_{nf} B^2(x)u, \tag{2}$$

$$u \frac{\partial T}{\partial x} + v \frac{\partial T}{\partial y} = \alpha_{nf} \frac{\partial^2 T}{\partial y^2} + \frac{\mu_{nf}}{(\rho C_p)_{nf}} \left( \frac{\partial u}{\partial y} \right)^2 - \frac{1}{(\rho C_p)_{nf}} \frac{\partial q_r}{\partial y} + \frac{q}{(\rho C_p)_{nf}} (T - T_\infty), \tag{3}$$

and the corresponding boundary conditions

$$u = U_w(x) = ax^n, \quad v = 0, \quad T = T_w = T_\infty + bx^{2n-1} \quad \text{at} \quad y = 0$$

$$u \rightarrow 0, \quad T = T_\infty \quad \text{as} \quad y \rightarrow \infty \tag{4}$$

where  $x$  is the direction along the sheet,  $y$  is the direction perpendicular to the sheet,  $u$  and  $v$  are the horizontal and vertical velocity in  $xy$ -direction respectively,  $\rho_{nf}$ ,  $\mu_{nf}$ ,  $(\rho C_p)_{nf}$ ,  $\beta_{nf}$ ,  $\sigma_{nf}$ ,  $k(x)$ ,  $\alpha_{nf} = \frac{k_{nf}}{(\rho C_p)_{nf}}$  and  $k_{nf}$  are respectively the effective density, coefficient of viscosity, heat capacitance at constant pressure, thermal expansion, electrical conductivity, variable permeability, thermal diffusivity and thermal conductivity of the nanofluids. While  $q_r$  and  $q$  are the radiative heat flux and heat generation constant respectively.

Under the usual Roseland approximation, the radiative heat flux is given by

$$q_r = -\frac{4\sigma^*}{3k^*} \frac{\partial T^4}{\partial y}, \tag{5}$$

where  $\sigma^*$  is the Stefan-Boltzmann constant and  $k^*$  is the mean absorption coefficient. The term  $T^4$  can be expressed as a linear function of temperature by assuming temperature difference within the flow region. Using Taylor's series expansion about the ambient temperature  $T_\infty$  and neglecting any higher order terms. The  $T^4$  can be expanded as

$$T^4 \cong 4T_\infty^3 T - 3T_\infty^4. \tag{6}$$

Following [6, 10, 30] the thermophysical properties of nanofluid are defined as

$$\rho_{nf} = (1 - \phi)\rho_f + \phi\rho_s, \tag{7}$$

$$\mu_{nf} = \frac{\mu_f}{(1 - \phi)^{2.5}}, \tag{8}$$

$$(\rho\beta)_{nf} = (1 - \phi)(\rho\beta)_f + \phi(\rho\beta)_s, \tag{9}$$

$$(\rho C_p)_{nf} = (1 - \phi)(\rho C_p)_f + \phi(\rho C_p)_s, \tag{10}$$

$$\frac{k_{nf}}{k_f} = \frac{(k_s + 2k_f) - 2\phi(k_f - k_s)}{(k_s + 2k_f) + \phi(k_f - k_s)}, \tag{11}$$

$$\frac{\sigma_{nf}}{\sigma_f} = 1 + \frac{3\left(\frac{\sigma_s}{\sigma_f} - 1\right)\phi}{\left(\frac{\sigma_s}{\sigma_f} + 2\right) - \left(\frac{\sigma_s}{\sigma_f} - 1\right)\phi}, \tag{12}$$

where  $\phi$ ,  $\rho_f$ ,  $\rho_s$ ,  $\mu_f$ ,  $\beta_f$ ,  $\beta_s$ ,  $(\rho C_p)_f$ ,  $(\rho C_p)_s$ ,  $\sigma_f$ ,  $\sigma_s$ ,  $k_f$  and  $k_s$  are respectively the nanoparticle solid volume fraction, the density of the pure fluid, the density of nanoparticle, the effective viscosity of the base fluid, the thermal expansion coefficient of the fluid, the thermal expansion coefficient of the nanoparticles, the heat capacitance of base fluid, the heat capacitance of nanoparticle, the electrical conductivity of the fluid, the electrical conductivity of the nanoparticles, the thermal conductivity of the base fluid and the thermal conductivity of the solid fraction.

The following non-dimensional similarity transformations were introduced in order to reduce the partial differential equations (2) and (3) into non-dimensional ordinary differential equations

$$\eta = \sqrt{\frac{(n+1)u}{2\nu x}} y, \quad \psi(x, y) = \sqrt{\frac{2\nu x}{(n+1)}} f(\eta),$$

$$\theta(\eta) = \frac{T - T_\infty}{T_w - T_\infty}, \tag{13}$$

where  $\eta(x, y)$  is the similarity variable,  $\nu$  is the kinematic viscosity of the fluid,  $\theta(\eta)$  dimensionless temperature and  $\psi(x, y)$  the stream function defined by

$$u = \frac{\partial \psi}{\partial y}, \quad v = -\frac{\partial \psi}{\partial x}. \tag{14}$$

By substituting Eqs. (5)–(12) into Eqs. (2) and (3), we have

$$f''' + (1 - \phi)^{2.5} \left(1 - \phi + \phi \frac{\rho_s}{\rho_f}\right) \left(f f'' - \left(\frac{2n}{n+1}\right) f'^2\right) - \left(\frac{2}{n+1}\right) \left\{ K + M(1 - \phi)^{2.5} \left[ 1 + \frac{3\left(\frac{\sigma_s}{\sigma_f} - 1\right)\phi}{\left(\frac{\sigma_s}{\sigma_f} + 2\right) - \left(\frac{\sigma_s}{\sigma_f} - 1\right)\phi} \right] \right\} f' = 0, \tag{15}$$

$$\frac{k_{nf}}{k_f} \left(1 + \frac{4}{3}R\right) \theta'' + Pr \left(1 - \phi + \phi \frac{(\rho C_p)_s}{(\rho C_p)_f}\right) \left\{ f \theta' - \left(\frac{2(2n-1)}{n+1}\right) f' \theta \right\} + Pr \left(\frac{Ec}{(1 - \phi)^{2.5}}\right) (f'')^2 + Pr \left(\frac{2}{n+1}\right) Q\theta = 0, \tag{16}$$

subject to the following non-dimensional conditions

$$f(\eta) = 0, \quad f'(\eta) = 1, \quad \theta(\eta) = 1 \quad \text{at} \quad \eta = 0$$

$$f'(\eta) = 0, \quad \theta(\eta) = 0 \quad \text{as} \quad \eta \rightarrow \infty. \tag{17}$$

The primes ( $'$ ) denote the derivative of a function  $f$  with respect to  $\eta$ ,  $\phi$  is the nanoparticle volume fraction,  $n$  is the nonlinear sheet parameter,  $M$  is the magnetic parameter,  $K$  is the permeability parameter,  $R$  is the radiation parameter,  $Pr$  is the Prandtl number,  $Ec$  is the Eckert number and  $Q$  is the heat generation parameter which are defined as

$$M = \frac{\sigma_f B_0^2}{\rho_f a}, \quad K = \frac{\nu_f}{ak_0}, \quad R = -\frac{4\sigma^* T_\infty^3 T}{k_{nf} k_{nf}^*},$$

$$Pr = \frac{\nu_f}{\alpha_f}, \quad Ec = \frac{U_w^2}{(c_p)_f (T_w - T_\infty)} \quad \text{and} \quad Q = \frac{qx}{(\rho c_p)_f U_w}. \tag{18}$$

The physical quantities of interests are the coefficient of skin friction  $C_f$  and the local Nusselt number  $Nu_x$ , which are defined by

$$C_f = \frac{\tau_w}{\rho_f u_w^2} \quad \text{and} \quad Nu_x = \frac{x q_w}{k_f (T_w - T_\infty)}, \tag{19}$$

where  $\tau_w$  is the skin friction from the plate and  $q_w$  is the wall heat flux from the plate. The wall skin friction and the heat flux in this problem are defined as

$$\tau_w = \mu_{nf} \left(\frac{\partial u}{\partial y}\right)_{y=0}$$

and

$$q_w = \left[ -\left(k_{nf} + \frac{16\sigma^* T_\infty^3}{3k^*}\right) \left(\frac{\partial T}{\partial y}\right) \right]_{y=0}. \tag{20}$$

Using the Eqs. (13), (14) and (20) in Eq. (19), the coefficient of the skin friction and the local Nusselt number can be expressed in terms of local Reynolds number  $Re_x = xu_x(x)/\nu_f$  as

$$Re_x^{1/2} C_f = \frac{1}{(1 - \phi)^{2.5}} \left(\frac{n+1}{2}\right)^{1/2} f''(0)$$

and

$$Re_x^{-1/2} Nu_x = -\frac{k_{nf}}{k_f} \left(1 + \frac{4}{3}R\right) \left(\frac{n+1}{2}\right)^{1/2} \theta'(0). \tag{21}$$

### 3. Method of solution

The Keller box method, which is an implicit finite difference scheme is employed to numerically solved the governing equations for this problem. The partial differential equations (1)–(3) governing the flow problem with the boundary conditions (4) are transformed into ordinary differential equations (15) and (16) with the corresponding boundary conditions (17). This method has four basic steps:

1. The transformed nonlinear ordinary differential equations (15) and (16) with the boundary condition (17) are written in terms of system of first order equations by introducing new independent variables  $f(\eta)$ ,  $u(\eta)$ ,  $v(\eta)$ ,  $r(\eta)$  and  $s(\eta)$ , defines as

$$f'(\eta) = u, \tag{22}$$

$$u'(\eta) = v, \tag{23}$$

$$r'(\eta) = s, \tag{24}$$

$$v' + (1 - \phi)^{2.5} \left( 1 - \phi + \phi \frac{\rho_s}{\rho_f} \right) \left( f v - \left( \frac{2n}{n+1} \right) u^2 \right) - \left( \frac{2}{n+1} \right) \left\{ K + M(1 - \phi)^{2.5} \left[ 1 + \frac{3 \left( \frac{\sigma_s}{\sigma_f} - 1 \right) \phi}{\left( \frac{\sigma_s}{\sigma_f} + 2 \right) - \left( \frac{\sigma_s}{\sigma_f} - 1 \right) \phi} \right] \right\} u = 0, \tag{25}$$

$$\frac{k_{nf}}{k_f} \left( 1 + \frac{4}{3} R \right) s' + Pr \left( 1 - \phi + \phi \frac{(\rho C_p)_s}{(\rho C_p)_f} \right) \left\{ f s - \left( \frac{2(2n-1)}{n+1} \right) u r \right\} + Pr \left( \frac{Ec}{(1-\phi)^{2.5}} \right) v^2 + Pr \left( \frac{2}{n+1} \right) Q r = 0, \tag{26}$$

where  $\theta(\eta) = r(\eta)$  and the corresponding boundary condition (17) becomes

$$f(\eta) = 0, \quad u(\eta) = 1 \quad \text{and} \quad r(\eta) = 1 : \quad \text{at} \quad \eta = 0, \\ u(\eta) \rightarrow 0, \quad v(\eta) \rightarrow 0 \quad \text{and} \quad r(\eta) \rightarrow 0 : \quad \text{as} \quad \eta \rightarrow \infty. \tag{27}$$

2. The first order equations obtained are then approximated about the mid point by the central differences at the mid points of the computational grid (mesh), and the function values are approximated as average, centred at the mid points of the mesh.
3. The approximated algebraic equations are linearized through Newton's method
4. The system of linearized equations are finally solved by the block-tridiagonal factorization method on the coefficient matrix of the finite difference equations.

The details of this Keller box techniques is found in the book of Cebeci and Bradshaw [31]. The numerical algorithms are developed using FORTRAN 77 for the iterative computation. In this problem, a step size  $\Delta\eta = 0.03$  was used in order to obtain the accurate numerical results and the convergence criterion is set to  $10^{-6}$  to achieve accuracy to six decimal places. The boundary layer thickness,  $\eta_\infty$  has been set at the range of 4 to 8, which defines the large values at which the satisfaction of the outer boundary condition is achieved.

#### 4. Results and discussion

In this article, we have studied the combine effects of thermal radiation, heat generation and viscous dissipation on magnetohydrodynamic nanofluid flow induced by a nonlinear stretching sheet using nanofluid model that incorporates nanoparticle volume fraction (i.e. Tiwari and Das model). The transformed ordinary differential equations (15) and (16) with the corresponding boundary conditions (17) are solved numerically through Keller box method. In order to get clear insight of the present problem, we investigate the effects of the governing physical parameters, namely nonlinear stretching parameter  $n$ , magnetic parameter  $M$ , permeability parameter  $K$ , nanoparticle volume fraction parameter  $\phi$ , Eckert number  $Ec$ , radiation parameter  $R$ , heat generation parameter  $Q$  and Prandtl number  $Pr$  on velocity and temperature profiles and at the same time the coefficient of skin friction and Nusselt number at the wall are also investigated and illustrated in Figs. 1, 2, 3, 4, 5, 6, 7, 8, 9, 10, 11, 12, 13, 14 and Table 2.

Figs. 1, 2, 3 and 4 show the behaviours of velocity and temperature profiles for various values of nanoparticle volume fraction  $\phi$  with

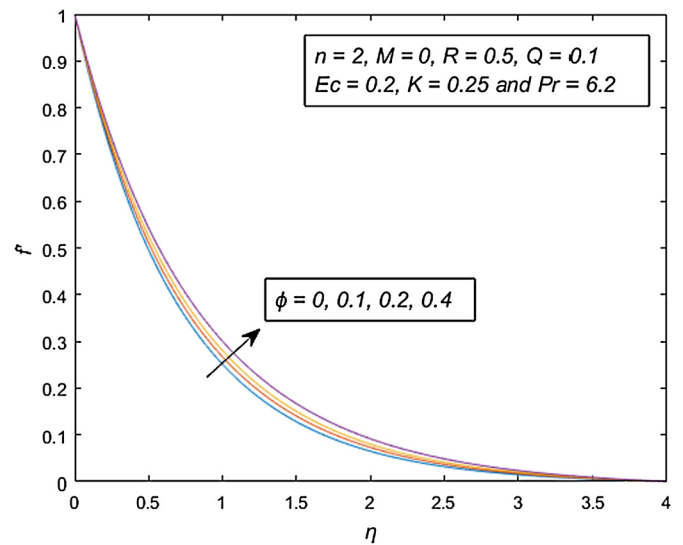


Fig. 1. Effect of nanoparticle volume fraction  $\phi$  on the velocity profile for  $M = 0$ .

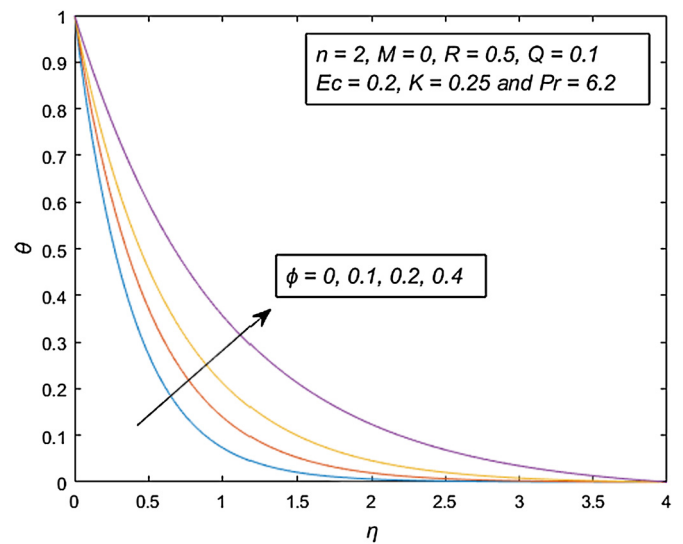


Fig. 2. Effect of nanoparticle volume fraction  $\phi$  on the temperature profile for  $M = 0$ .

and without magnetic field  $M$ . It is evident from these figures that horizontal velocity increased with an increase in the value of nanoparticle volume fraction. This implies that an increase in  $\phi$  weakens the flow and leads to the rise in the thickness of momentum boundary layer. Similarly, temperature profiles are enhanced with the increased in the nanoparticle volume fraction. This is due to the fact that the thermal conductivity of nanofluid rises with the suspension of more solid particles into the based fluid which in turns increases the heat transfer. This increase in the temperature profiles leads to the increase in the thermal boundary layer thickness. However, the thermal boundary layer become thicker as the values of  $\phi$  increases from 0 (i.e. water) to 0.4 (i.e. Cu-water). This is due to the fact that copper posses higher thermal conductivity as compared to the conventional based fluid. It is also observed from these figures that the effect of magnetic field on the nanoparticle volume fraction is higher with respect to the temperature profiles as compared to the velocity profiles for the same values of  $\phi$ .

Figs. 5 and 6 illustrate the effects of permeability parameter  $K$  on the velocity field and the temperature distribution. We infer from these figures that the velocity profile decreases with the increased in the porosity parameter  $K$ . This arises due to the fact that an increase

**Table 2**

Variations of skin friction coefficient  $-f''(0)$  and Nusselt number  $-\theta'(0)$  for various values of dimensionless governing parameters.

$\phi$	$n$	$M$	$K$	$R$	$Q$	$Ec$	$Pr$	$-f''(0)$	$-\theta'(0)$
0.0	2.0	2.0	1.0	0.5	0.1	0.2	6.2	2.925685	1.071278
0.1	2.0	2.0	1.0	0.5	0.1	0.2	6.2	2.702822	0.851237
0.2	2.0	2.0	1.0	0.5	0.1	0.2	6.2	2.453807	0.684889
0.1	1.0	2.0	1.0	0.5	0.1	0.2	6.2	3.110913	0.007866
0.1	3.0	2.0	1.0	0.5	0.1	0.2	6.2	2.551360	1.198705
0.1	7.0	2.0	1.0	0.5	0.1	0.2	6.2	2.368892	1.642800
0.1	2.0	1.0	1.0	0.5	0.1	0.2	6.2	2.263951	1.154667
0.1	2.0	3.0	1.0	0.5	0.1	0.2	6.2	3.057832	0.610651
0.1	2.0	4.0	1.0	0.5	0.1	0.2	6.2	3.359251	0.413473
0.1	2.0	2.0	0.0	0.5	0.1	0.2	6.2	2.496834	0.993365
0.1	2.0	2.0	1.0	0.5	0.1	0.2	6.2	2.702822	0.851237
0.1	2.0	2.0	4.0	0.5	0.1	0.2	6.2	3.214060	0.507483
0.1	2.0	2.0	1.0	0.2	0.1	0.2	6.2		1.001576
0.1	2.0	2.0	1.0	0.5	0.1	0.2	6.2		0.851237
0.1	2.0	2.0	1.0	1.0	0.1	0.2	6.2		0.696058
0.1	2.0	2.0	1.0	0.5	0.0	0.2	6.2		0.957718
0.1	2.0	2.0	1.0	0.5	0.5	0.2	6.2		0.614231
0.1	2.0	2.0	1.0	0.5	1.0	0.2	6.2		0.337540
0.1	2.0	2.0	1.0	0.5	0.1	0.1	6.2		1.193353
0.1	2.0	2.0	1.0	0.5	1.1	0.3	6.2		0.509122
0.1	2.0	2.0	1.0	0.5	1.1	0.5	6.2		0.175110
0.1	2.0	2.0	1.0	0.5	0.1	0.2	5.0		0.748020
0.1	2.0	2.0	1.0	0.5	1.1	0.2	7.0		0.915389
0.1	2.0	2.0	1.0	0.5	1.1	0.2	9.0		1.059447

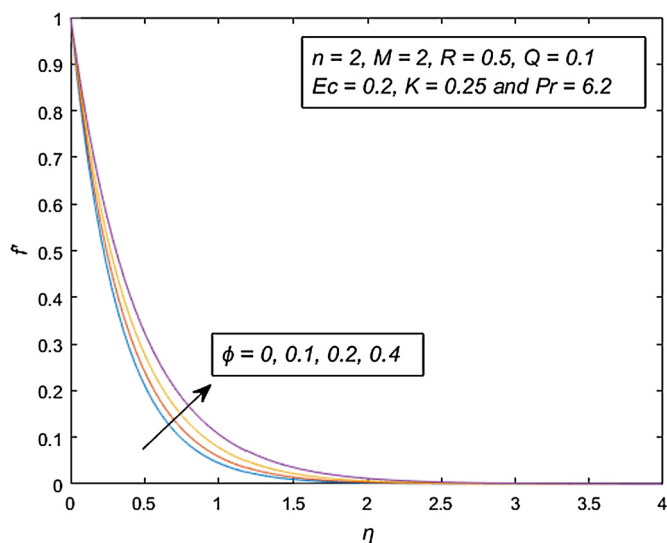


**Fig. 3.** Effect of nanoparticle volume fraction  $\phi$  on the velocity profile for  $M = 2$ .

in  $K$  amplify the porous layer and thereby reduces the thickness of momentum boundary layer. Likewise, an increase in  $K$  enhances the temperature distributions in the boundary layer region. Physically, that heat is being transferred from the solid wall to the flow region by Darcian's body force.

Figs. 7 and 8 show the influence of nonlinear stretching sheet parameter  $n$  on velocity and temperature profiles. It can be observed from Fig. 7 that there is an increase in the velocity profile for larger values of  $n$ . This enhancement in the non-dimensional stretching velocity is due to larger value of  $n$  and it tends to produce more deformation in the liquid. This phenomenon shows that the associated momentum boundary layer become thicker as the value of  $n$  increases. Whereas a decrease in the temperature profile is noticed with an increased in  $n$ , thereby leading to the increase in the heat transfer.

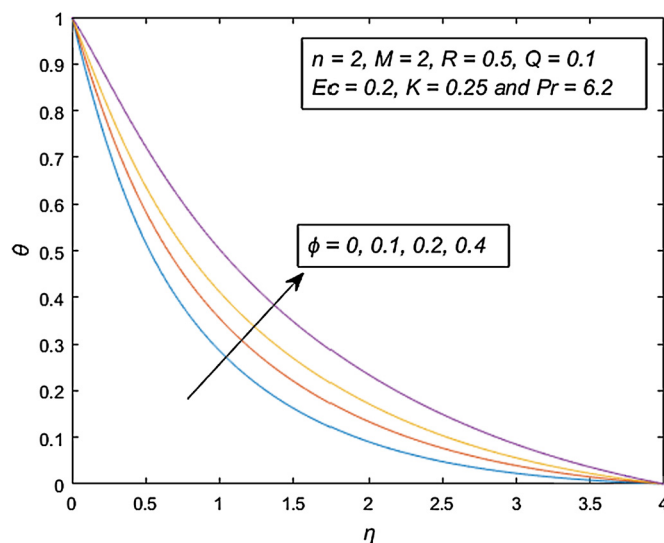


**Fig. 4.** Effect of nanoparticle volume fraction  $\phi$  on the temperature profile for  $M = 2$ .

Variations of various values of heat generation parameter  $Q$  on the temperature profile is displayed in Fig. 9. It is obvious that heat generation takes place in the thermal boundary layer whenever  $Q$  increases positively. The intense amount of heat generated in the fluid leads to enhancement of the thermal energy of the nanofluid. This process escalates the thermal boundary layer thickness which implies that heat energy is released and thereby leads to the increase in the fluid's temperature.

The variation of Eckert number  $Ec$  with the temperature profile is depicted in Fig. 10. The presence of Eckert number in nanofluid raises the production of thermal energy which become more intense which leads to the enhancement in the temperature distributions and consequently thermal layer thickness. This is due to the fact that the viscosity of nanofluid stores energy from the flow due to the increase in heat en-

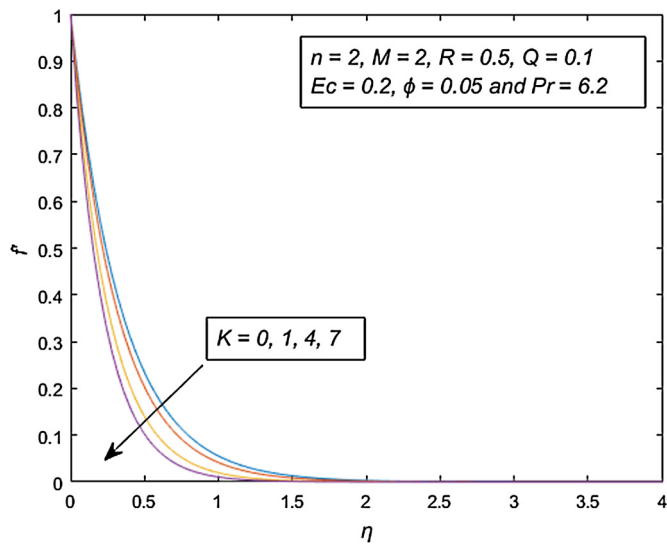


Fig. 5. Effect of permeability parameter  $K$  on the velocity profile.

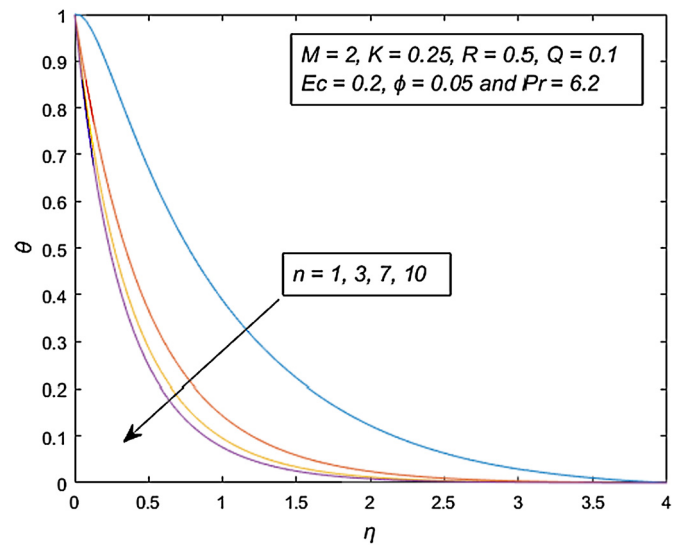


Fig. 8. Effect of nonlinear stretching parameter  $n$  on the temperature profile.

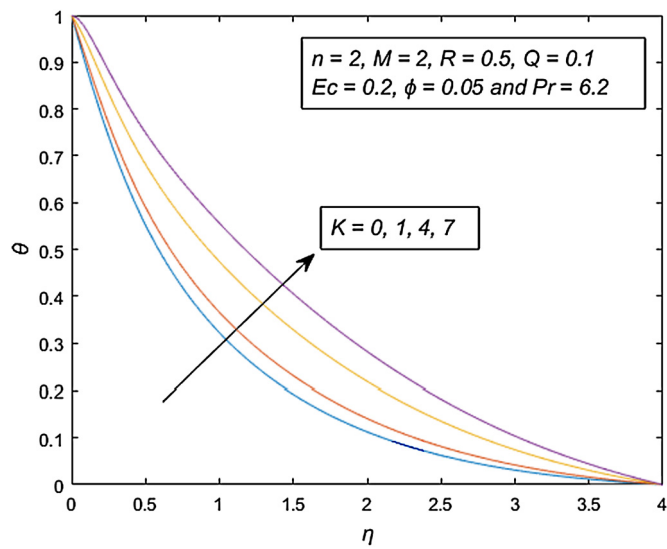


Fig. 6. Effect of permeability parameter  $K$  on the temperature profile.

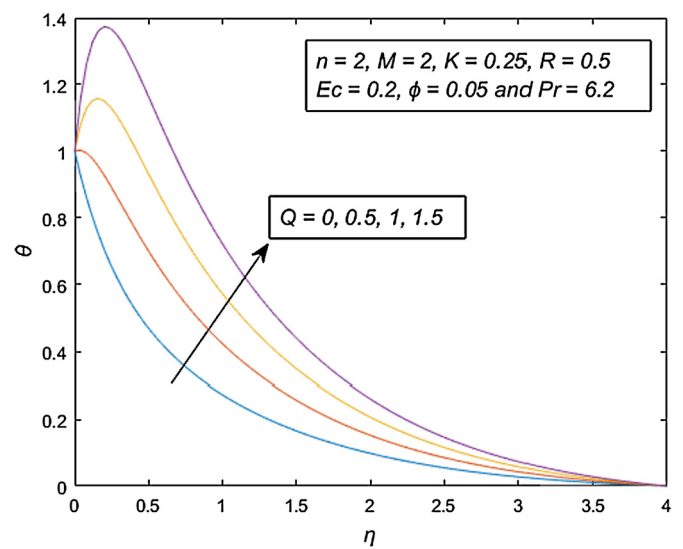


Fig. 9. Effect of heat generation parameter  $Q$  on the temperature profile.

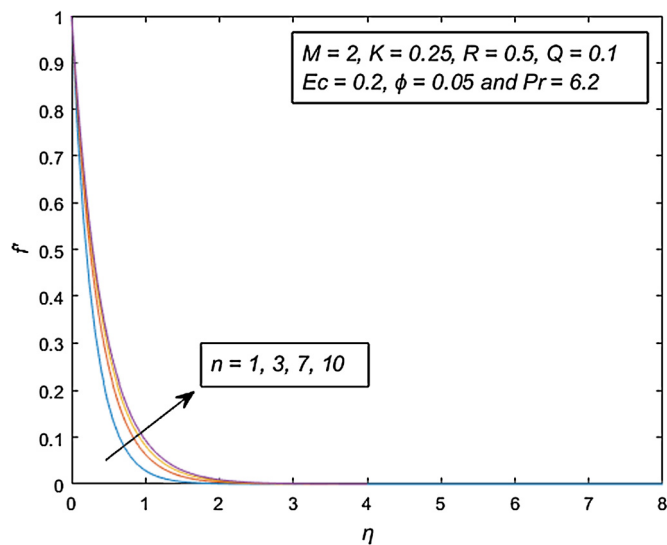


Fig. 7. Effect of nonlinear stretching parameter  $n$  on the velocity profile.

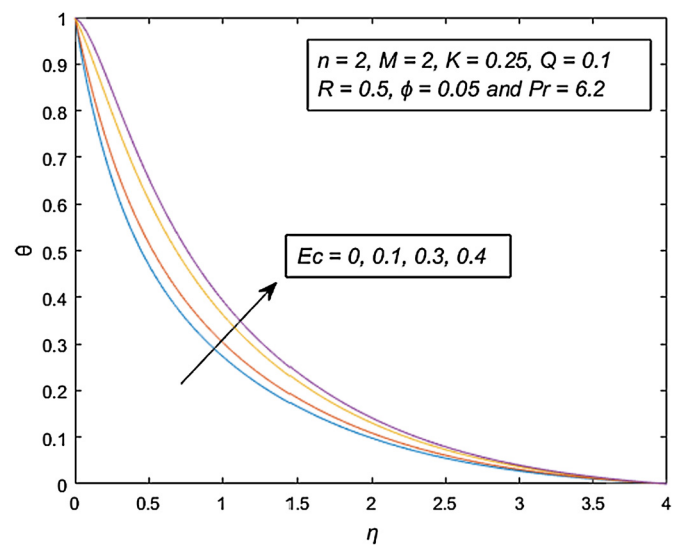


Fig. 10. Effect of Eckert number  $Ec$  on the temperature profile.

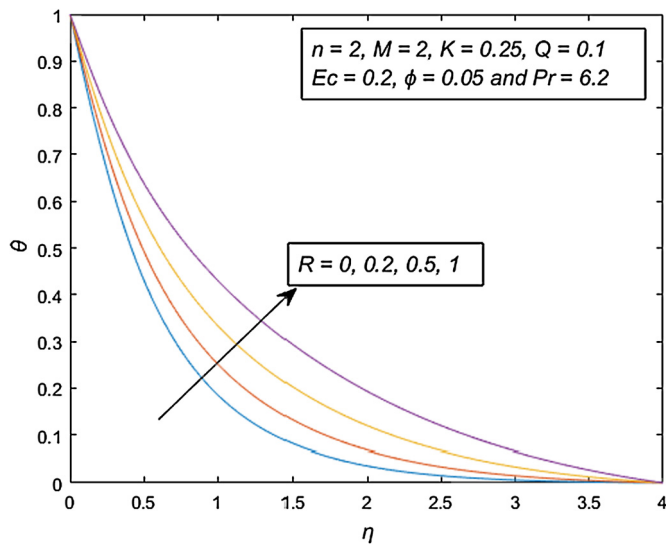


Fig. 11. Effect of radiation parameter  $Q$  on the temperature profile.

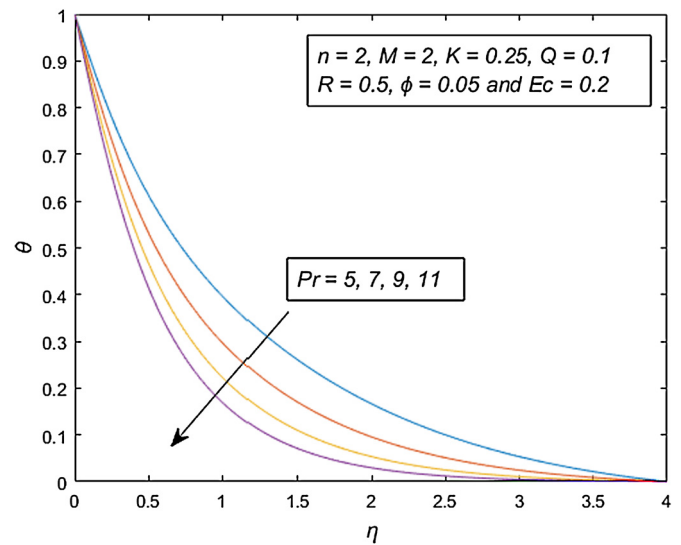


Fig. 14. Effect of Prandtl number  $Pr$  on the temperature profile.

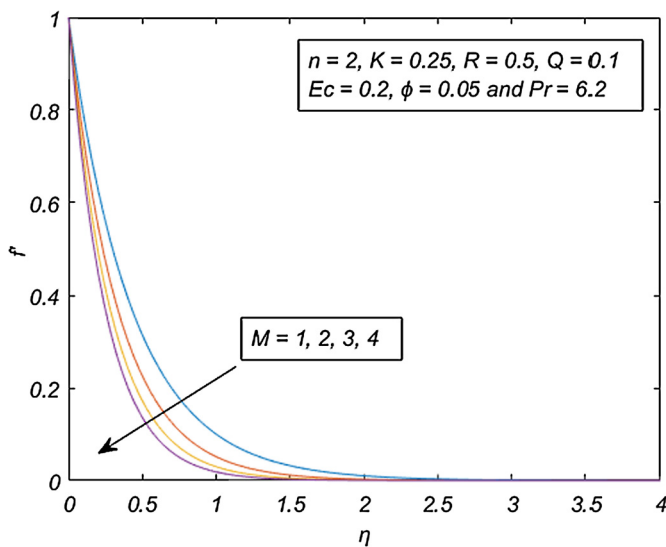


Fig. 12. Effect of magnetic parameter  $M$  on the velocity profile.

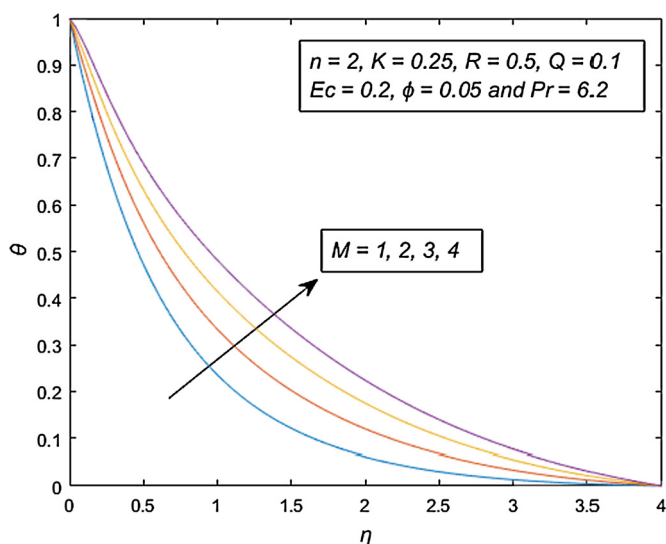


Fig. 13. Effect of magnetic parameter  $M$  on the temperature profile.

ergy by frictional heating and transforms it into internal energy where the nanofluid thermal energy gain heated.

The effect of thermal radiation on temperature distribution is illustrated in Fig. 11. It is observed that temperature distribution increases with the increase in the thermal radiation parameter  $R$ . An increment in the radiation parameter causes fluid to release heat energy from the flow region which prompts the temperature of the nanofluid to rise and thereby cools the system. Large value of radiation parameter produces more heat to the system which eventually escalate the temperature of the fluid and thereby increases the thickness of thermal boundary layer. This is apparent that mean absorption coefficient  $k^*$  decays with its increase which may be responsible for the increase of thermal field. The presence of magnetic field also influences the rises in the temperature. This shows that the thermal radiation should be at minimal value for a better cooling process.

The effect of magnetic parameter  $M$  on velocity and temperature profiles are exhibited in Figs. 12 and 13. Here, we noticed that the velocity profile is a decreasing function of  $M$  whereas temperature profile escalate with the increase in  $M$ . Interestingly, a stronger magnetic force gives more resistance to the flow of nanofluid. As a result of the decrease in the velocity profile, the momentum boundary layer thickness declined as shown in Fig. 12. While the thickness of the thermal boundary layer rises as the Lorentz force in the magnetic field becomes stronger with higher values of  $M$ . It is obvious that magnetic field produces an opposing/resistive force known as Lorentz force which reduces the velocity of the fluid and prompt the flow boundary layer to be become thinner. Furthermore, as the temperature profile enhanced, the thermal boundary layer thickness increased.

The behaviour of temperature profile for various values of Prandtl number  $Pr$  is depicted in Fig. 14. It is clearly seen from this figure that an increase in  $Pr$  reduces the temperature profiles which resulted in the decrease in the thermal boundary layer thickness. This implies that heat will diffuse quickly for larger values of Prandtl number. Thus, the thermal diffusivity of the fluid grows as the Prandtl number increases which leads to the enhancement of the temperature of the fluid.

To ascertain the accuracy of the current results, the comparison of the present results with the previous results of Hady et al. [11] for local Nusselt number  $-\theta(0)$  are shown in Table 3. The comparison affirms a good and close agreement as displayed in the table. Table 2 displays the impact of flow parameters,  $n, \phi, M, K, R, Q, Ec$  and  $Pr$  on the coefficient of skin friction and the local Nusselt number for the mixture of Copper nanoparticle and the water as based fluid. It is evident from this table that the magnitude of coefficient of skin friction is enhanced with the increased in magnetic and porosity parameters, whereas an in-

**Table 3**

Comparison of Nusselt number at the wall for the present results and that of Hady et al. [11] when  $K = R = Q = 0$  and  $n = Pr = 1$ .

$Ec$	$n$	$-\theta'(0)$	$-\theta'(0)$
		Hady et al. [11]	Present results
0.0	0.75	3.123518	3.1231
	1.5	3.566532	3.5660
	7.0	4.184386	4.1846
	10	4.254939	4.2539
0.1	0.75	3.013524	3.0134
	1.5	3.453154	3.4539
	7.0	4.063757	4.0635
	10	4.133338	4.1331

crease in  $\phi$  and  $n$  leads to the decrease in the coefficient of skin friction. In the same vein, an increased in local Nusselt number is also observed by augmenting the values of  $n$  and  $Pr$ , while an increase in  $\phi$ ,  $M$ ,  $K$ ,  $R$ ,  $Q$  and  $Ec$  reduces the values of local Nusselt number, which implies that nanofluid will be of importance in heating and cooling process.

## 5. Conclusion

The influence of combined effects of heat generation parameter, radiation parameter, nanoparticle volume fraction and Eckert number on magnetohydrodynamic flow of nanofluid past a nonlinear stretching sheet saturated in a porous medium is numerically studied. The partial differential equations govern the fluid flow and heat transfer are transformed into system of fourth order ordinary differential equations via a suitable similarity transformation which are then solved with the aid Keller box method. The study revealed how the behaviour of the governing parameters such as nonlinear stretching parameter  $n(1, 3, 7, 10)$ , nanoparticle volume fraction  $\phi(0, 0.1, 0.2, 0.4)$ , permeability parameter  $K(0, 1, 4, 7)$ , magnetic parameter  $M(1, 2, 3, 4)$ , radiation parameter  $R(0, 0.2, -0.5, 1)$ , heat generation parameter  $Q(0, 0.5, 1, 1.5)$ , Eckert number  $Ec(0, 0.1, 0.3, 0.4)$  and Prandtl number  $Pr(5, 7, 9, 11)$  affect the nanofluid flow and the characteristics of heat transfer problems. The following summary were made from the current study:

- An increase in the value of nanoparticle volume fractions  $\phi$  enhances the velocity field and the temperature distribution in the thermal layer region.
- An increase in the value of Eckert number, heat generation parameter and radiation parameter increases the fluid's temperature.
- An enhancement of thermal boundary layer is observed with the rise in the porosity parameter.
- The coefficient skin friction escalate with the rise in  $M$ ,  $K$ , and reduces with  $n$  and  $\phi$ , whereas the rate of heat transfer at the surface reduces by intensifying the values of  $\phi$ ,  $M$ ,  $K$ ,  $Ec$ ,  $Q$ ,  $R$ , and intensify with the rise in  $n$  and  $Pr$ .

## Declarations

### Author contribution statement

Ahmad Banji Jafar: Conceived and designed the analysis; Analyzed and interpreted the data; Wrote the paper.

Sharidan Shafie and Imran Ullah: Analyzed and interpreted the data; Wrote the paper.

### Funding statement

The authors would like to acknowledge Ministry of Education (MOE) and Research Management Centre-UTM, Universiti Teknologi Malaysia (UTM) for the financial support through vote numbers 5F004, 07G70, 07G72, 07G76 and 07G77 for this research.

## Competing interest statement

The authors declare no conflict of interest.

## Additional information

No additional information is available for this paper.

## References

- [1] S.U.S. Choi, Enhancing thermal conductivity of fluids with nanoparticles in developments and applications of Non-Newtonian flows FED-vol. 231/MD 66, 1995 pp. 99-105.
- [2] M. Goyal, R. Bhargava, Boundary layer flow and heat transfer of viscoelastic nanofluids past a stretching sheet with partial slip conditions, *Appl. Nanosci.* 4 (2014) 761-767.
- [3] Y. Xuan, L. Qiang, Heat transfer enhancement of nanofluids, *Int. J. Heat Fluid Flow* 2 (2000) 58-64.
- [4] S.U.S. Choi, Z.G. Zhang, W. Yu, F.E. Lockwood, E.A. Grulke, Anomalous thermal conductivity enhancement in nanotube suspensions, *Appl. Phys. Lett.* 79 (2001) 2252-2254.
- [5] J. Buongiorno, Convective transport in nanofluids, *J. Heat Transf.* 128 (2006) 240-250.
- [6] R.K. Tiwari, M.K. Das, Heat transfer augmentation in a two-sided lid-driven differentially heated square cavity utilizing nanofluids, *Int. J. Heat Mass Transf.* 50 (2007) 2002-2018.
- [7] J. Yang, L. Feng-Chen, W. Zhou, Y. He, B. Jiang, Experimental investigation on the thermal conductivity and shear viscosity of viscoelastic-fluid-based nanofluids, *Int. J. Heat Mass Transf.* 55 (2012) 3160-3166.
- [8] W.A. Khan, I. Pop, Boundary-layer flow of a nanofluid past a stretching sheet, *Int. J. Heat Mass Transf.* 53 (2010) 2477-2483.
- [9] P. Rana, B. Rama, Finite element simulation of transport phenomena of viscoelastic nanofluid over a stretching sheet with energy dissipation, *J. Inf. Oper. Manag.* 3 (2012) 212-226.
- [10] M.A.A. Hamad, M. Ferdows, Similarity solutions to viscous flow and heat transfer of nanofluid over nonlinearly stretching sheet, *Appl. Math. Mech.* 33 (2012) 923-930.
- [11] F.M. Hady, F.S. Ibrahim, S.M. Abdel-Gaied, M.R. Eid, Radiation effect on viscous flow of a nanofluid and heat transfer over a nonlinearly stretching sheet, *Nanoscale Res. Lett.* 7 (2012) 229-242.
- [12] K. Das, Nanofluid flow over a non-linear permeable stretching sheet with partial slip, *J. Egypt. Math. Soc.* 23 (2015) 451-456.
- [13] J.A. Khan, M. Mustafa, T. Hayat, A. Alsaedi, Three-dimensional flow of nanofluid over a non-linearly stretching sheet: an application to solar energy, *Int. J. Heat Mass Transf.* 86 (2015) 158-164.
- [14] A. Malvandi, F. Hedayati, D.D. Ganji, Nanofluid flow on the stagnation point of a permeable non-linearly stretching/shrinking sheet, *Alex. Eng. J.* 57 (2017) 2199-2208.
- [15] S.U. Khan, S.A. Shehzad, Brownian movement and thermophoretic aspects in third-grade nanofluid over oscillatory moving sheet, *Phys. Scr.* 94 (2019) 095202.
- [16] M.H. Matin, M. Dehsara, A. Abbassi, Mixed convection MHD flow of nanofluid over a non-linear stretching sheet with effects of viscous dissipation and variable magnetic field, *Mechanics* 18 (2012) 415-423.
- [17] A. Zare, M. Javad, M. Hemmat, Nanofluid implementation for heat transfer augmentation of magneto hydrodynamic flows in a lid-driven cavity using experimental-based correlations, *Int. J. Appl. Electromagn. Mech.* 42 (2013) 589-602.
- [18] N. Sandeep, C. Sulochana, C.S.K. Raju, M.J. Babu, Unsteady boundary layer flow of thermophoretic MHD nanofluid past a stretching sheet with space and time dependent internal heat source/sink, *Appl. Math.* 10 (2015) 312-327.
- [19] S. Naramgari, C. Sulochana, Dual solutions of radiative MHD nanofluid flow over an exponentially stretching sheet with heat generation/absorption, *Appl. Nanosci.* 6 (2016) 131-139.
- [20] M. Khan, M. Azam, Unsteady heat and mass transfer mechanisms in MHD Carreau nanofluid flow, *J. Mol. Liq.* 225 (2017) 554-562.
- [21] A. Jamaludin, R. Nazar, I. Pop, Three-dimensional magnetohydrodynamic mixed convection flow of nanofluids over a nonlinearly permeable stretching/shrinking sheet with velocity and thermal slip, *Appl. Sci.* 8 (2018) 1128.
- [22] I. Ahmad, M. Sajid, W. Awan, M. Rafique, W. Aziz, M. Ahmed, A. Abbasi, M. Taj, MHD flow of a viscous fluid over an exponentially stretching sheet in a porous medium, *J. Appl. Math.* (2014) 1-7.
- [23] Z. Shah, E. Bonyah, S. Islam, W. Khan, M. Ishaq, Radiative MHD thin film flow of Williamson fluid over an unsteady permeable stretching sheet, *Heliyon* 4 (2018) e00825.
- [24] A. Zeeshan, R. Ellahi, M. Hassam, Magnetohydrodynamic flow of water/ethylene glycol based nanofluids with natural convection through porous medium, *Eur. Phys. J. Plus* 129 (2014) 261-271.
- [25] D. Pal, G. Mandal, Mixed convection-radiation on stagnation-point flow of nanofluids over a stretching/shrinking sheet in a porous medium with heat generation and viscous dissipation, *J. Pet. Sci. Eng.* 126 (2015) 16-25.

- [26] R. Bhargava, H. Chandra, Numerical simulation of MHD boundary layer flow and heat transfer over a nonlinear stretching sheet in the porous medium with viscous dissipation using hybrid approach, arXiv preprint, arXiv:1711.03579, 2017.
- [27] N.A.H. Haroun, S. Mondal, P. Sibanda, Hydromagnetic nanofluids flow through a porous medium with thermal radiation, chemical reaction and viscous dissipation using the spectral relaxation method, *Int. J. Comput. Methods* 16 (2017) 1840020.
- [28] Y. Geng, A. Hassan, M. Monfared, R. Moradi, MHD nanofluid heat transfer between a stretching sheet and a porous surface using neural network approach, *Int. J. Mod. Phys. C* 30 (2019) 1950048.
- [29] H.R. Patel, Effects of cross diffusion and heat generation on mixed convective MHD flow of Casson fluid through porous medium with non-linear thermal radiation, *Heliyon* 5 (2019) e01555.
- [30] M. Sheikholeslami, M. Hatami, D.D. Ganji, Nanofluid flow and heat transfer in a rotating system in the presence of a magnetic field, *J. Mol. Liq.* 190 (2014) 112–120.
- [31] T. Cebeci, P. Bradshaw, *Physical and Computational Aspects of Convective Heat Transfer*, Springer Sc. Bus. Media, 2012.